

A study of characteristic element length for higher-order finite elements

*Original*

A study of characteristic element length for higher-order finite elements / Shen, Jiahui. - (2023). ( III Aerospace PhD-Days International Congress of PhD Students in Aerospace Science and Engineering Bertinoro, Forli (ITA) 16-19 April 2023,).

*Availability:*

This version is available at: 11583/3004540 since: 2025-10-28T12:26:39Z

*Publisher:*

AIDAA

*Published*

DOI:

*Terms of use:*

This article is made available under terms and conditions as specified in the corresponding bibliographic description in the repository

*Publisher copyright*

(Article begins on next page)

# A STUDY OF CHARACTERISTIC ELEMENT LENGTH FOR HIGHER-ORDER FINITE ELEMENTS

Jiahui Shen<sup>1,a\*</sup>

<sup>1</sup> Politecnico di Torino, Corso Duca degli Abruzzi 24, 10129 Torino, Italy

<sup>a</sup>jiahui.shen@polito.it

**Keywords:** Fracture energy regularization; Characteristic element length; Damage analysis; Higher-order beam theories; Carrera unified formulation;

**Abstract.** The utilization of a fracture energy regularization technique, based on the crack band model, can effectively resolve the issue of mesh-size dependency in the finite element modelling of quasi-brittle structures. However, achieving accurate results requires proper estimation of the characteristic element length in the finite element method. This study presents practical calculation methods for the characteristic element length, particularly for higher-order finite elements based on the Carrera Unified Formulation (CUF). Additionally, a modified Mazars damage model that incorporates fracture energy regularization is employed for damage analysis in quasi-brittle materials. An experimental benchmark is adopted then for validation, and the result shows that the proposed methods ensure accurate regularization of fracture energy and provide mesh-independent structural behaviors.

## 1 Introduction

Higher-order beam finite element method based on Carrera unified formulation (CUF) [1] allows for one-dimensional analysis along the beam direction, with three-dimensional results obtained by expanding the cross-section using different polynomials such as Taylor [2] and Lagrange [3, 4]. The Lagrange expansion is a popular choice for many engineering analyses due to its ability to fit well with arbitrary cross-sections. However, when considering the strain-softening behavior of quasi-brittle materials, where stress decreases as strain increases, achieving mesh objectivity in the numerical results poses a significant challenge in finite element analyses.

The objectivity of numerical results in the framework of continuum mechanics can be restored by various regularization methods, such as integral-type or gradient-type nonlocal models [5, 6], viscous or rate-dependent methods [7], and the crack band approach [8] (or fracture energy regularization method). Among them, the crack band approach is a popular analytical tool due to its simplicity and efficiency. It can give mesh-independent finite element (FE) results by regularizing the softening curves of Gaussian points according to the crack bandwidth during calculation. Therefore, the key parameter in this method is the crack bandwidth (or characteristic element length).

The crack bandwidth is influenced by many characteristics of finite elements such as the shape, the order, the dimension, the interpolation function and scheme, and so on [9]. Over the past decades, several estimations for crack bandwidth have been proposed and can be categorized into three groups: (1) methods based on the square root of the element area or cubic root of the element volume [10]; (2) projection methods or methods proposed by Govindjee [11]; and (3) methods



proposed based on Oliver [12]. However, all the above methods are applicable to two-dimensional or linear elements, which is not suitable for higher-order finite elements. Some researchers have made many modifications based on the previous three methods such as adding influencing factors to consider the element order [13, 14], which will also inspire this work. In this work, two methods will be proposed and discussed by comparing results from a numerical benchmark.

## 2 Finite elements based on CUF

This work is based on the higher-order beam theories within the framework of CUF, as described in [1]. To maintain brevity and simplicity, only the essential framework is presented here. The 1D unified formulation can be expressed as follows:

$$\mathbf{u}(x, y, z) = F_\tau(x, z)\mathbf{u}_\tau(y), \quad \tau = 1, 2, \dots, M \quad (1)$$

where  $y$  is set as the axial direction;  $(x, z)$  creates the cross-section plane;  $F_\tau(x, z)$  varies within the cross-section;  $\mathbf{u}_\tau(y)$  is the generalized displacement vector;  $\tau$  represents the summation;  $M$  stands for the number of terms in the expansion.

In this work, Lagrange-like polynomials are adopted as cross-section expanding functions  $F_\tau$ , which is known as the Lagrange expansion (LE). The quadrilateral element with different orders such as four-node bilinear (L4), nine-node quadratic (L9) and sixteen-node cubic (L16) is mainly utilized. As an illustration, the interpolation function for L4 is shown as an example:

$$F_\tau = \frac{1}{4}(1 + rr_\tau)(1 + ss_\tau), \quad \tau = 1, 2, 3, 4 \quad (2)$$

where  $(r, s)$  are natural coordinates that vary from -1 to 1 and  $r_\tau$  and  $s_\tau$  are the actual coordinates.

The classical beam shape functions can be adopted to approximate the generalized displacement field  $\mathbf{u}_\tau$  and Eq. 1 can be rewritten as:

$$\mathbf{u}(x, y, z) = F_\tau(x, z)N_i(y)\mathbf{u}_{\tau i}, \quad i = 1, 2, \dots, N_{NE} \quad (3)$$

where  $N_i$  is the shape functions of classical beam elements including two nodes (B2), three nodes (B3), and four nodes (B4) for choice;  $N_{NE}$  is the number of nodes per element;  $\mathbf{u}_{\tau i}$  is the nodal displacement vector.

## 3 Modified Mazars damage model

Mazars [15] proposed a simple isotropic damage model considering a scalar damage variable which can be written as:

$$\boldsymbol{\sigma} = (1 - d)\mathbf{E}_0\boldsymbol{\varepsilon} \quad (4)$$

where  $\boldsymbol{\sigma}$  and  $\boldsymbol{\varepsilon}$  represent stress and strain, respectively;  $\mathbf{E}_0$  is the stiffness matrix of undamaged material;  $d$  is the damage variable.

More details on modified Mazars damage models can be found in [16]. For explaining fracture energy regularization, the tensile damage evolution law is presented here:

$$d_t = \begin{cases} 1 - \frac{\varepsilon_{d0}}{\kappa_t} \exp\left(\frac{\varepsilon_{d0} - \kappa_t}{\varepsilon_{tu} - \varepsilon_{d0}}\right) & \text{if } \kappa_t \leq \varepsilon_{tres} \\ 1 - \frac{p_t \times \varepsilon_{d0}}{\kappa_t} & \text{if } \kappa_t > \varepsilon_{tres} \end{cases} \quad (5)$$

where  $\varepsilon_{d0}$  is the maximum strain of elastic period;  $\kappa_t$  is a internal variable for loading function which is the equivalent strain in Mazars damage model;  $p_t$  is defined as the ratio between the residual tensile stress and uniaxial tensile strength which ensures the damage is infinitely close to 1.0 but not equals 1.0;  $\varepsilon_{tres}$  is the residual strain corresponding to the residual stress;  $\varepsilon_{tu}$  is the equivalent ultimate strain for bilinear softening, which is relevant to the constitutive law.

The fracture energy regularization technique is employed for controlling the slope of the softening diagram which is related to  $\varepsilon_{tu}$ . It can be realized by the following equation:

$$\frac{G_f}{l_c} = f_{ctm}(\varepsilon_{tu} - \varepsilon_{d0}) \quad (6)$$

where  $G_f$  is the fracture energy of the material;  $f_{ctm}$  is the tensile strength;  $l_c$  is the crack bandwidth or characteristic element length.

#### 4 Crack bandwidths estimation

The first method developed for higher-order finite elements was proposed in [10], which is based on the cubic root of the element volume. The volume consists of one beam element and one Lagrange element, as shown in Fig. 1 for further clarification. The element volume is the product of beam element length  $l_e$  and Lagrange element area  $A_e$ , and can be divided into smaller elements based on the order of the beam and Lagrange elements. In Fig. 1, the element volume is divided into eight smaller elements, and the crack bandwidth can be estimated by taking the cubic root of the smaller volume. Therefore, the crack bandwidth can be estimated using the following equation:

$$l_{p1} = \sqrt[3]{\frac{l_e \times A_e}{(\sqrt{M}-1)^2 \times (N_{NE}-1)}} \quad (7)$$

However, this method requires that the smaller volume shown in Fig. 1 should be cubical. Therefore, the following equation should be approximately satisfied:

$$\frac{\sqrt{A_e}}{l_e} \approx \frac{\sqrt{M}-1}{N_{NE}-1} \quad (8)$$

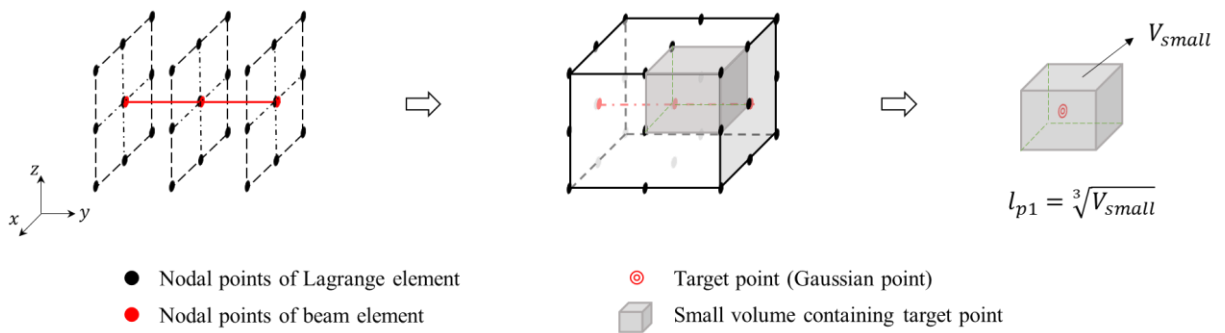


Figure 1. Description of method 1

The other method is inspired by [9, 13] which reported that strain localization with softening only occurs on some Gaussian points within a single higher-order element, rather than all of them. This phenomenon is attributed to the influence of the element order. The method estimates the crack bandwidths as follows:

$$l_{p2} = l_g \times \alpha \quad (9)$$

where  $l_g$  is the estimated length from [11] and  $\alpha$  can be considered as a correction factor for the strain localization.

For a clear explanation, Fig. 2 illustrates the calculation process after assembling a cube element and conducting a 3D Govindjee's projection. Then the Gaussian points are divided into three layers, as L9 is adopted, with 9 Gaussian points in each layer due to the use of B3. In the first layer, two-thirds of the Gaussian points undergo softening, suggesting a value of  $\alpha$  as 13/18. In the second layer, all Gaussian points undergo softening, so  $\alpha$  is 1.0. In the third layer, all Gaussian points are still in elastic linear period and no damage is detected. It is worth noting that the suggested value of  $\alpha$  is from [9, 13], which is actually from the weight ratio of softening Gaussian points to all Gaussian points on one element. But in this CUF based higher-order beam elements,  $\alpha$  is suggested as the weight ratio of softening Gaussian points to all Gaussian points on one specific layer, illustrating  $\alpha$  is not always the same for all Gaussian points in this higher-order beam theory.

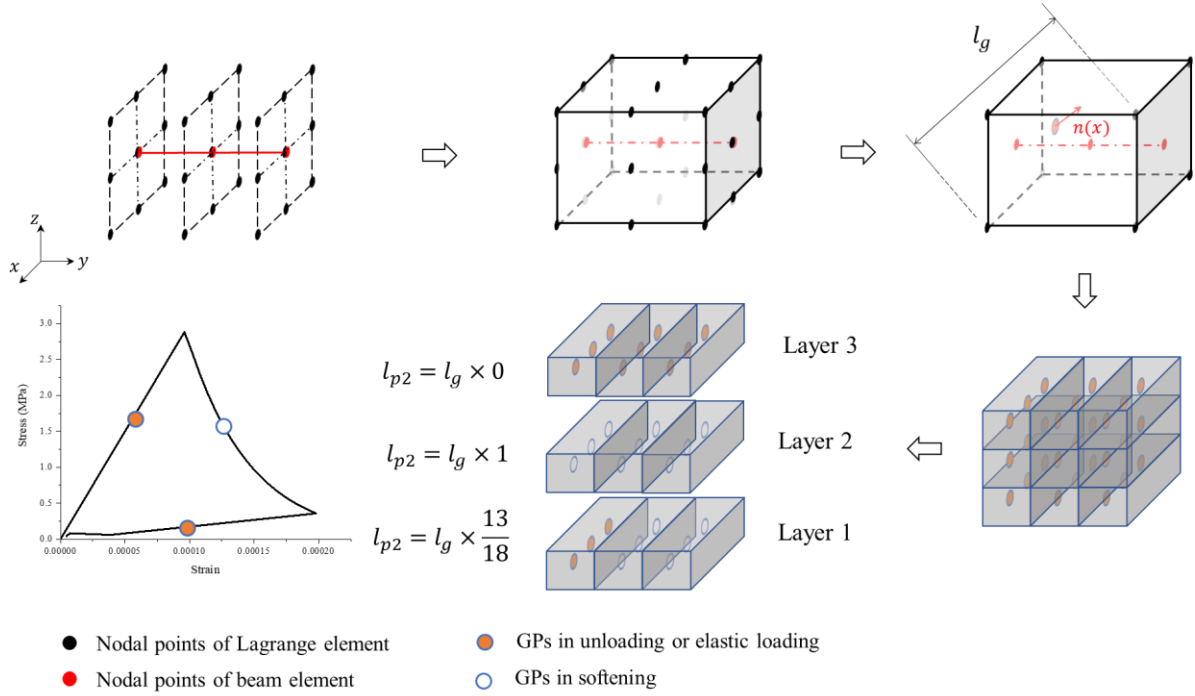


Figure 2. Description of method 2

## 5 Numerical examples

The present study utilizes the Hassanzadeh test [17], which is a benchmark direct tension test for quasi-brittle materials, to compare and validate proposed methods. Fig. 3 shows the dimension of a cube sample with four edges notched in the middle. The bottom is fixed and a tension is imposed on the top via displacement control. The material is concrete, with an elastic modulus of 36 GPa, a tensile strength of 3.5 MPa, and a Poisson's ratio of 0.2.

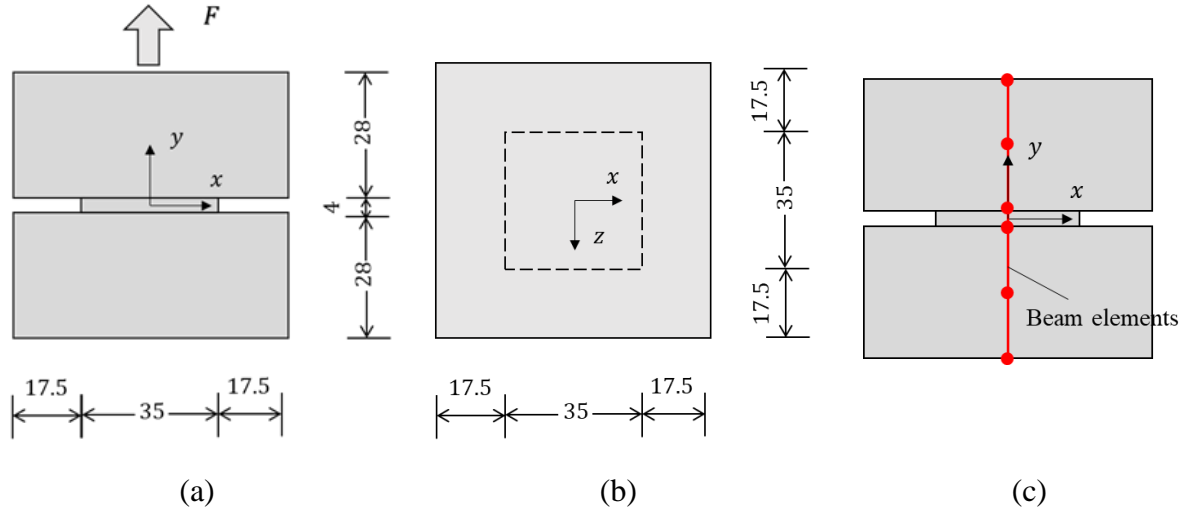


Figure 3. Information of test sample (unit: mm): (a) Front view, (b) Top view, and (c) Assignment of beam elements

Figure. 3(c) illustrates the assignment of beam elements, which are used in the present study. Various numbers and orders of beam elements are considered, as shown in Table 1. The configuration of Lagrange elements for all models will be consistent, using L9 elements with the same size.

Table 1: Model information

Model No.	Model 1	Model 2	Model 3	Model 4	Model 5	Model 6
Beam Configuration	1B2+4B2	2B2+4B2	1B3+4B3	2B3+4B3	1B4+2B4	2B4+2B4
Total DoFs	6498	6681	11193	11919	9390	10479

All load-displacement curves of different models obtained from different methods are plotted in Fig. 4. When two beam elements are adopted in the middle notch, Method 1 fails to provide results due to non-convergence. Additionally, when B4 elements are adopted, the peak load and softening part of the curve are both lower than other models, suggesting that Method 1 is unable to regularise the fracture energy because Eq. 8 is not satisfied. From Fig. 4(b), Method 2 provides great results that all models producing similar curves except for Model 6 which has a slightly lower curve. This indicates Method 2 provides a reliable estimation of crack bandwidths, successfully preserving the fracture energy.

The damage distribution of all models obtained using different methods are shown in Fig. 5. For models with Method 1, the damage distributions that limited to the notched part are reasonable. However, when B3 or B4 elements are adopted for Method 2, some issues arise, resulting in the fracture area extending beyond the middle notched part. Nevertheless, the damage intensity is not too significant.

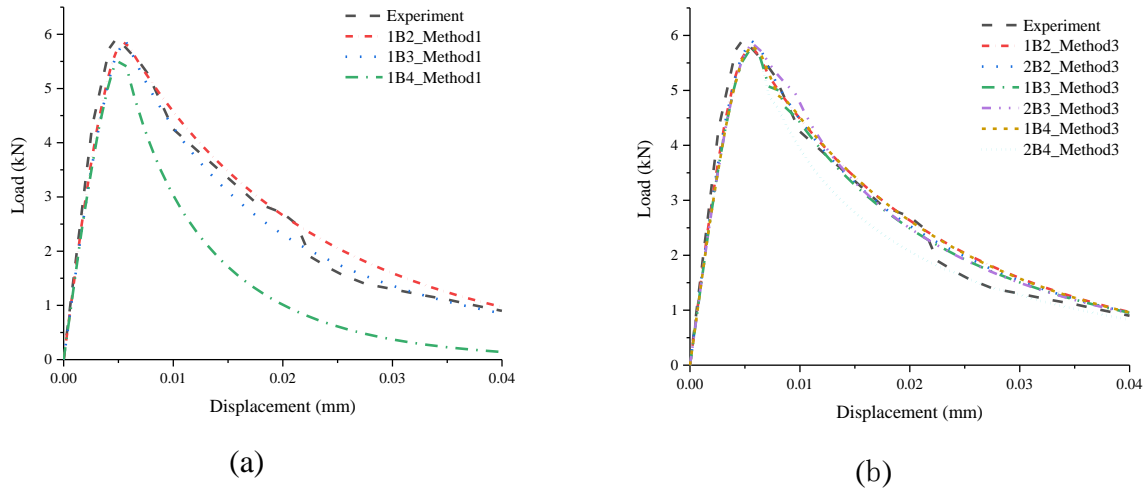


Figure 4: Load-displacement curves from: (a) Method 1 and (b) Method 2

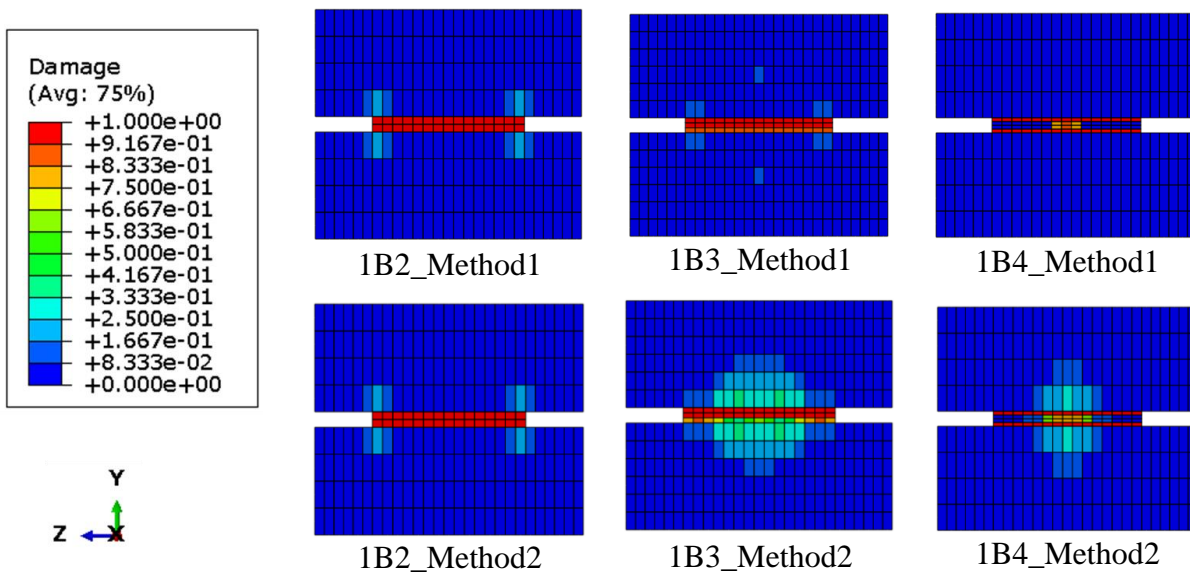


Figure 5: Damage distribution of different models from different methods

## 6 Conclusions

This work shows the damage analysis of quasi-brittle materials using CUF-based higher-order finite elements. A modified Mazars damage model with fracture energy regularization is utilized. Two methods are proposed for estimating the crack bandwidths or characteristic element length, which is a crucial parameter for fracture energy regularization in higher-order beam elements. While Method 2 yielded the best performance in the previous analysis, both methods provide objective structural behaviors that are mesh independent and can help preserve fracture energy to some extent.

## Reference

- [1] M Petrolo, E Carrera, M Cinefra, E Zappino. Finite element analysis of structures through unified formulation. John Wiley & Sons, 2014. <https://doi.org/10.1002/9781118536643.index>
- [2] E Carrera, M Filippi, E Zappino. Laminated beam analysis by polynomial, trigonometric, exponential and zig-zag theories. *European Journal of Mechanics-A/Solids* 41 (2013): 58-69. <https://doi.org/10.1016/j.euromechsol.2013.02.006>
- [3] A Pagani, E Carrera, R Augello, D Scano. Use of Lagrange polynomials to build refined theories for laminated beams, plates and shells. *Composite Structures* 276 (2021): 114505. <https://doi.org/10.1016/j.compstruct.2021.114505>
- [4] J Shen, A Pagani, MRT Arruda, E Carrera. Exact component-wise solutions for 3D free vibration and stress analysis of hybrid steel–concrete composite beams. *Thin-Walled Structures* 174 (2022): 109094. <https://doi.org/10.1016/j.tws.2022.109094>
- [5] G Pijaudier-Cabot, ZP Bažant. Nonlocal damage theory. *Journal of engineering mechanics* 113.10 (1987): 1512-1533. [https://doi.org/10.1061/\(ASCE\)0733-9399\(1987\)113:10\(1512\)](https://doi.org/10.1061/(ASCE)0733-9399(1987)113:10(1512))
- [6] EC Aifantis. On the role of gradients in the localization of deformation and fracture. *International Journal of Engineering Science* 30.10 (1992): 1279-1299. [https://doi.org/10.1016/0020-7225\(92\)90141-3](https://doi.org/10.1016/0020-7225(92)90141-3)
- [7] G Duvant, JL Lions. *Inequalities in mechanics and physics*. Vol. 219. Springer Science & Business Media, 2012. <http://dx.doi.org/10.1007/978-3-642-66165-5>
- [8] ZP Bažant, BH Oh. Crack band theory for fracture of concrete. *Matériaux et construction* 16 (1983): 155-177. <https://doi.org/10.1007/BF02486267>
- [9] M Jirásek, M Bauer. Numerical aspects of the crack band approach. *Computers & structures* 110 (2012): 60-78. <https://doi.org/10.1016/j.compstruc.2012.06.006>
- [10] J Shen, MRT Arruda, A Pagani. Concrete damage analysis based on higher-order beam theories using fracture energy regularization. *Mechanics of Advanced Materials and Structures* (2022): 1-15. <https://doi.org/10.1080/15376494.2022.2098430>
- [11] S Govindjee, GJ Kay, JC Simo. Anisotropic modelling and numerical simulation of brittle damage in concrete. *International journal for numerical methods in engineering* 38.21 (1995): 3611-3633. <https://doi.org/10.1002/nme.1620382105>
- [12] J Oliver. A consistent characteristic length for smeared cracking models. *International Journal for Numerical Methods in Engineering* 28.2 (1989): 461-474. <https://doi.org/10.1002/nme.1620280214>
- [13] AT Slobbe, MAN Hendriks, JG Rots. Systematic assessment of directional mesh bias with periodic boundary conditions: Applied to the crack band model. *Engineering Fracture Mechanics* 109 (2013): 186-208. <https://doi.org/10.1016/j.engfracmech.2013.06.005>
- [14] W He, Y Xu, Y Cheng, PF Jia, TT Fu. Tension-compression damage model with consistent crack bandwidths for concrete materials. *Advances in Civil Engineering* 2019 (2019). <https://doi.org/10.1155/2019/2810108>
- [15] J Mazars. Application de la mécanique de l'endommagement au comportement non linéaire et à la rupture du béton de structure. THESE DE DOCTEUR ES SCIENCES PRESENTÉE A L'UNIVERSITÉ PIERRE ET MARIE CURIE-PARIS 6 (1984).

[16] MRT Arruda, J Pacheco, LMS Castro, E Julio. A modified mazars damage model with energy regularization. *Engineering Fracture Mechanics* 259 (2022): 108129. <https://doi.org/10.1016/j.engfracmech.2021.108129>

[17] M Hassanzadeh. Behaviour of fracture process zones in concrete influenced by simultaneously applied normal and shear displacements. Division of Building Materials, Lund Institute of Technology, 1992.